Effects of *mono*- or *di*-fluoro-substitution on spin crossover behaviour in a pair of Schiff base Fe^{II}-coordination Polymer

Yu Luo [a#], Ren-He Zhou [a#], Zhen Shao [a], Dan Liu [a], Han-Han Lu [a], Meng-Jia Shang [a], Liang Zhao *[a], Tao Liu [a], Yin-Shan Meng *[a]

[a] *State Key Laboratory of Fine Chemicals, Frontier Science Center for Smart Materials, School of Chemical Engineering, Dalian University of Technology, 2 Linggong Road, Dalian 116024, China.*

*Corresponding authors. E-mail: zhaoliang716@dlut.edu.cn (L. Zhao), mengys@dlut.edu.cn (Y. S. Meng)

Contents

Experimental section.

All reagents were commercially available and used without further purification. H_2L and $FeL(MeOH)_2$ were synthesized according to a procedure in the literature.

Synthesis of organic ligand L_1 (2,3-FDPB):

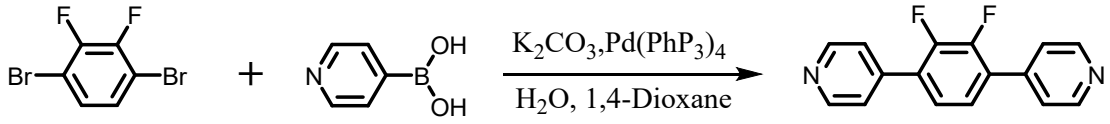

4-pyridylboronic acid (1.35 g, 11 mmol), potassium carbonate (2.54 g, 18 mmol), and Pd (PPh_3) $_4$ (0.50 g, 0.433mmol) were added to the reaction flask, and 1,4-dibromo-2,3-difluorobenzene (1.0g, 3.7mmo1) was added under N_2 protection. A mixture of solvent water and 1,4-dioxane (10mL of water, 20mL of 1,4-dioxane) was added to the reaction flask. The mixture was stirred and heated to 90 ℃, and reacted for 72 hours to obtain the reaction product mixture. The mixture was cooled to room temperature and concentrated under reduced pressure. The concentrated solution of the reaction product was extracted three times with ethyl acetate (20 mL each time). The organic layer was dried with anhydrous $MgSO_4$ and the solvent was removed to obtain the crude product. The crude product was separated by using a silicone chromatography column (the eluent is a mixture of petroleum ether and ethyl acetate, with a volume ratio of 2:1), and obtained a white solid 4 '- (2,5-difluoro-1,4-phenylene) dipyridine 0.7 g (with a yield of 35. 14%).^{1}H NMR(500 MHz, $CDCl_3$): δ 8.78-8.72(m, 4H), 7.58-7.50(m, 4H), 7.40-7.33(m,2H). Anal. Calcd (%) for $\mathbf{L}_1$: C, 76.79; H, 4.43; N, 11.19. Found: C, 76.92; H, 4.51; N, 11.35.

Synthesis of organic ligand L_2 (2 - FDPB):

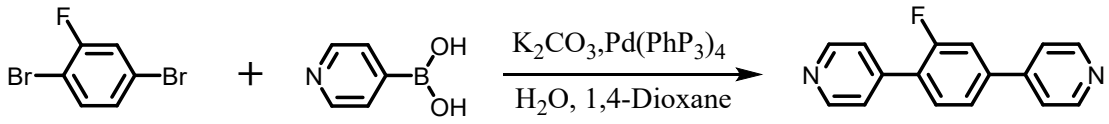

1,4-dibromo-2-difluorobenzene (0.93 g, 3.7 mmo1), 4-pyridylboronic acid (1.35 g, 11 mmo1), potassium carbonate (2.54 g, 18 mmol) and Pd (PPh_3) $_4$ (0.50 g, 0.433 mmol) were added to the reaction flask under N_2 protection, respectively. A mixture solution of water and 1,4-dioxane (10mL water, 20 mL 1,4-dioxane) was added to the reaction flask. The mixture was stirred and heated to 90 ℃, and reacted for 72 hours to obtain the reaction product mixture. The mixture was cooled to room temperature and concentrated under reduced pressure. The concentrated solution of the reaction product was extracted three times with ethyl acetate (20 mL each time). The organic layer was dried with anhydrous $MgSO_4$ and the solvent was removed to obtain the crude product. The crude product was separated by using a silicone chromatography column (the eluent is a mixture of petroleum ether and ethyl acetate, with a volume ratio of 2:1), and obtained a white solid 4 '- (2-fluoro-1,4-phenylene) dipyridine 0.6 g (with a yield of 40.52%). ^{1}H NMR(500 MHz, CDCl3): δ 8.76-8.68(m, 4H), 7.64-7.46(m,7H). Anal. Calcd (%) for $\mathbf{L}_2$: C, 71.64; H, 3.76; N, 10.44. Found: C, 71.80; H, 3.89; N, 10.68.

Table S1. Crystallographic data of complexes

Complex	**1**		**2**
Temperature, K	120	300	120
CCDC	2347760	2347761	2347771
Formula	$C_{36.25}H_{30.5}Cl_{0.5}F_4FeN_4O_6$		$C_{72.5}H_{64}F_6Fe_2N_8O_{12.5}$
Formula weight	767.72		1473.01
Crystal system	monoclinic		triclinic
Space group	$P2_1/n$	$P2_1/n$	$P\bar{1}$
a/Å	15.418(2)	15.877(2)	12.217(5)
b/Å	12.9986(18)	13.1330(16)	13.650(8)
c/Å	17.693(2)	17.844(2)	23.294(9)
α/°	90	90	97.356(15)
β/°	99.066(3)	95.284(4)	93.002(12)
γ/°	90	90	107.035(17)
Volume/Å^3	3501.6(8)	3705.0(8)	3667(3)
Z	4	4	2
ρ_{calc}g/cm^3	1.456	1.338	1.334
F(000)	1578	1536	1522
Reflections collected	61483	78147	83808
Goodness-of-fit on F^2	1.068	1.040	1.036
R_1 $[I \geq 2\sigma(I)]$[a]	0.0443	0.0668	0.0897
wR_2 $[I \geq 2\sigma(I)]$[b]	0.1124	0.1957	0.2439

[a] $R_1 = \Sigma\ (|F_o|-|F_c|) / \Sigma\ |F_o|$; [b] $wR_2 = [\Sigma\ w\ (|F_o|-|F_c|)^2 / \Sigma\ w\ F_o^2]^{1/2}$

Table S2. Selected bond lengths (Å) for **1** at different temperatures

	120 K	300 K
	Length (Å)	Length (Å)
Fe1–O1	1.9307(15)	2.033(3)
Fe1–O2	1.9420(14)	2.009(3)
Fe1–N1	1.9046(17)	2.109(3)
Fe1–N2	1.9084(17)	2.107(3)
Fe1–N3	1.9838(17)	2.227(3)
Fe1–N4	1.9977(17)	2.260(2)

Table S3. Selected bond lengths (Å) for **2** at 120 K

	120 K
	Length(Å)
Fe1–O1	1.936(4)
Fe1–O2	1.927(4)
Fe1–N1	1.905(5)
Fe1–N2	1.900(5)
Fe1–N3	1.988(5)
Fe1–N4[2]	1.992(5)
Fe2–O3	1.941(4)
Fe2–O4	1.942(4)
Fe2–N5	1.906(5)
Fe2–N6	1.899(5)
Fe2–N7	2.002(5)
Fe2–N8[1]	2.005(5)

Table S4. Selected bond angles (º) for **1** at different temperatures.

Complex	**1**	
Temperature (K)	120	300
O1–Fe1–O2	87.93(6)	111.27(11)
O1–Fe1–N1	93.70(7)	84.77(11)
O1–Fe1–N2	177.91(7)	163.45(11)
O1–Fe1–N3	88.53(6)	87.69(10)
O1–Fe1–N4	87.40(6)	85.68(10)
O2–Fe1–N1	178.25(7)	163.62(11)
O2-Fe1-N2	93.25(7)	85.28(11)
O2–Fe1–N3	88.72(6)	91.01(10)
O2–Fe1–N4	87.37(6)	88.36(10)
N1–Fe1–N2	85.15(7)	78.73(11)
N1–Fe1–N3	91.98(7)	93.00(10)
N1–Fe1–N4	92.04(7)	89.65(10)
N2–Fe1–N3	89.77(7)	91.86(10)
N2–Fe1–N4	94.37(7)	95.44(10)
N3–Fe1–N4	174.47(7)	172.60(10)
Σ_{Fe}	30.46	62.42
$CShM_{Fe}$	0.183	1.479

Table S5. Selected bond angles (º) for **2** at 120 K.

Complex		**2**	
Temperature (K)		120	
O1–Fe1–O2	87.34(17)	O3-Fe2-O4	89.03(17)
O1–Fe1–N1	93.43(19)	O3-Fe2-N5	92.61(18)
O1–Fe1–N2	178.85(19)	O3-Fe2-N6	177.72(18)
O1–Fe1–N3	88.85(18)	O3-Fe2-N7	87.57(18)
O1–Fe1–N4[2]	88.84(18)	O3-Fe2-N8[1]	89.48(18)
O2–Fe1–N1	178.73(19)	O4-Fe2-N5	177.09(19)
O2–Fe1–N2	93.78(19)	O4-Fe2-N6	92.95(19)
O2–Fe1–N3	88.91(18)	O4-Fe2-N7	87.35(18)
O2–Fe1–N4[2]	87.92(18)	O4-Fe2-N8[1]	91.04(18)
N1–Fe1–N2	85.5(2)	N5-Fe2-N6	85.4(2)
N1–Fe1–N3	92.1(2)	N5-Fe2-N7	90.32(19)
N1–Fe1–N4[2]	91.1(2)	N5-Fe2-N8	91.37(19)
N2–Fe1–N3	90.9(2)	N6-Fe2-N7	93.6(2)
N2–Fe1–N4[2]	91.5(2)	N6-Fe2-N8	89.4(2)
N3–Fe1–N4[2]	176.16(19)	N7-Fe2-N8	176.67(18)
Σ_{Fe}	25.50	Σ_{Fe}	23.64
$CShM_{Fe}$	0.136	$CShM_{Fe}$	0.156

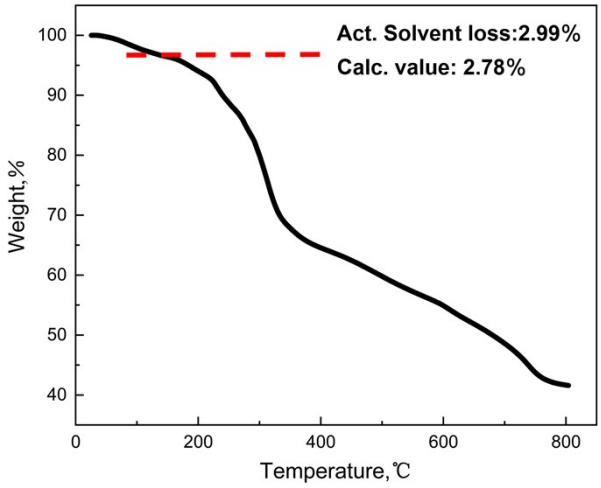

Fig. S1 TGA curve for complex **1** in N_2 atmosphere with a heating rate of 10 $K \cdot min^{-1}$.

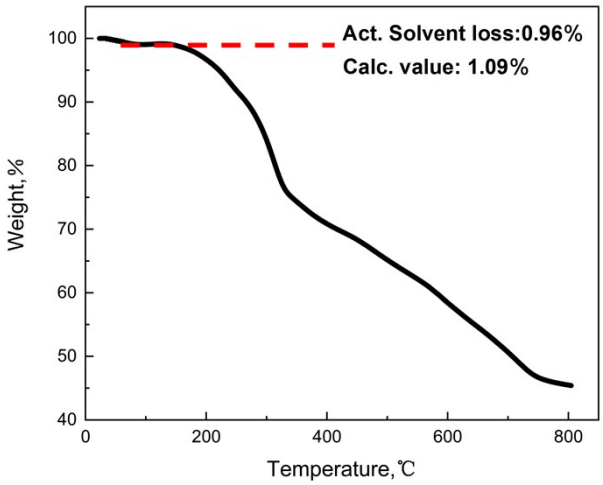

Fig. S2 TGA curve for complex **2** in N_2 atmosphere with a heating rate of 10 K·min^{-1}.

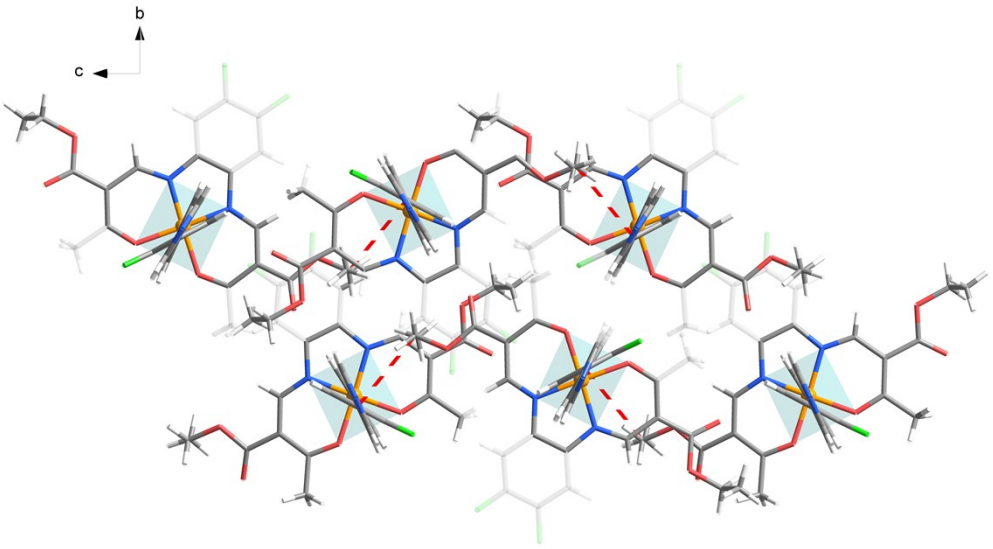

Fig. S3 The intermolecular C–H···π between adjacent chains and molecular packing of **1**

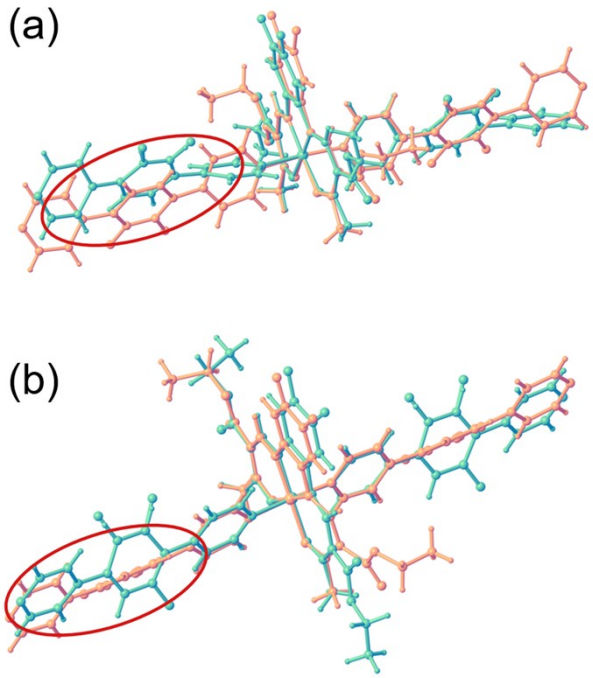

Fig. S4 Overlay map of **1** and **2.** a) Fe1 of **2**, b) Fe2 of **2**

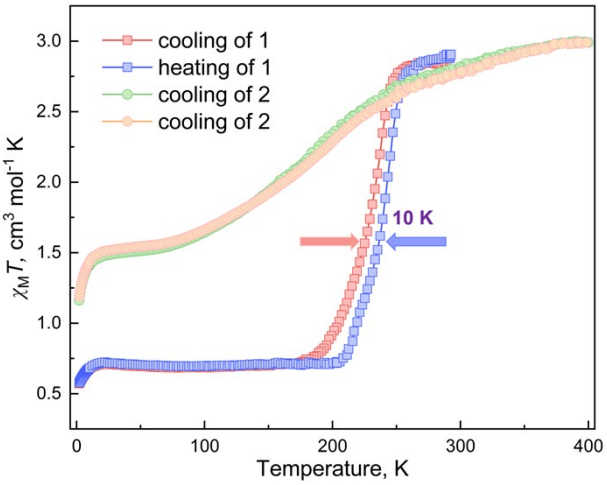

Fig. S5 Plots of the temperature dependence of $\chi_M T$ under 1 kOe dc field for complexes after loss solvent (a) **1**, (b) **2**. Fresh samples contained in the plastic capsule were heated to 120° for 5 hours under the nitrogen atmosphere. The nitrogen atmosphere was replaced every half hour to ensure that the solvents were completely removed.

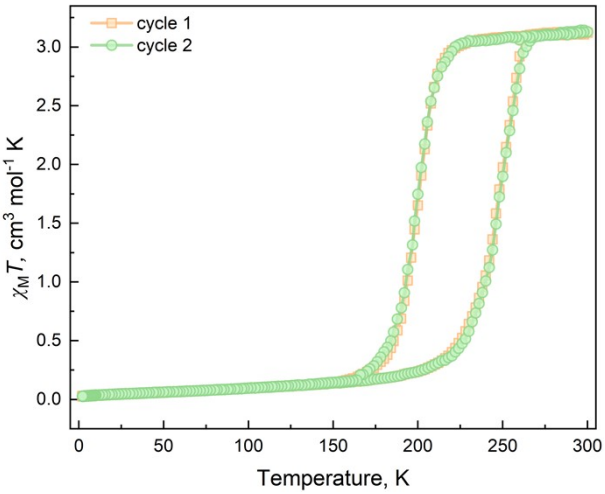

Fig. S6 Temperature-dependent susceptibilities of **1** with the temperature-sweeping rate of 3 K/min over the temperature range of 2-300 K. The $\chi_M T$ vs. T curves were repeated well, confirming that the solvent was well retained.

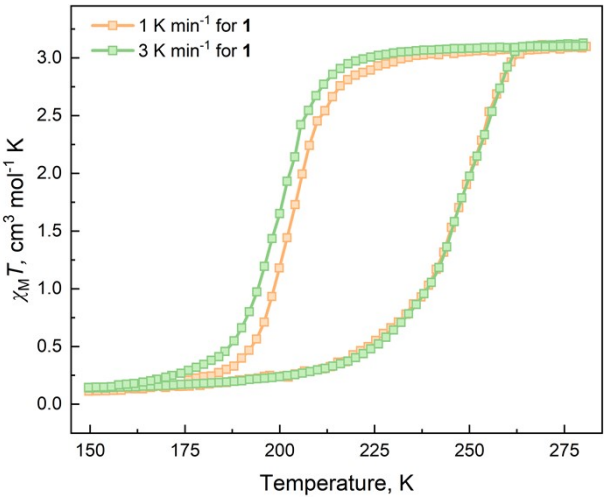

Fig. S7 Scan rate study of temperature-dependent susceptibilities of **1** with the temperature-sweeping rates of 1 and 3 K/min over the temperature range of 150-280 K.

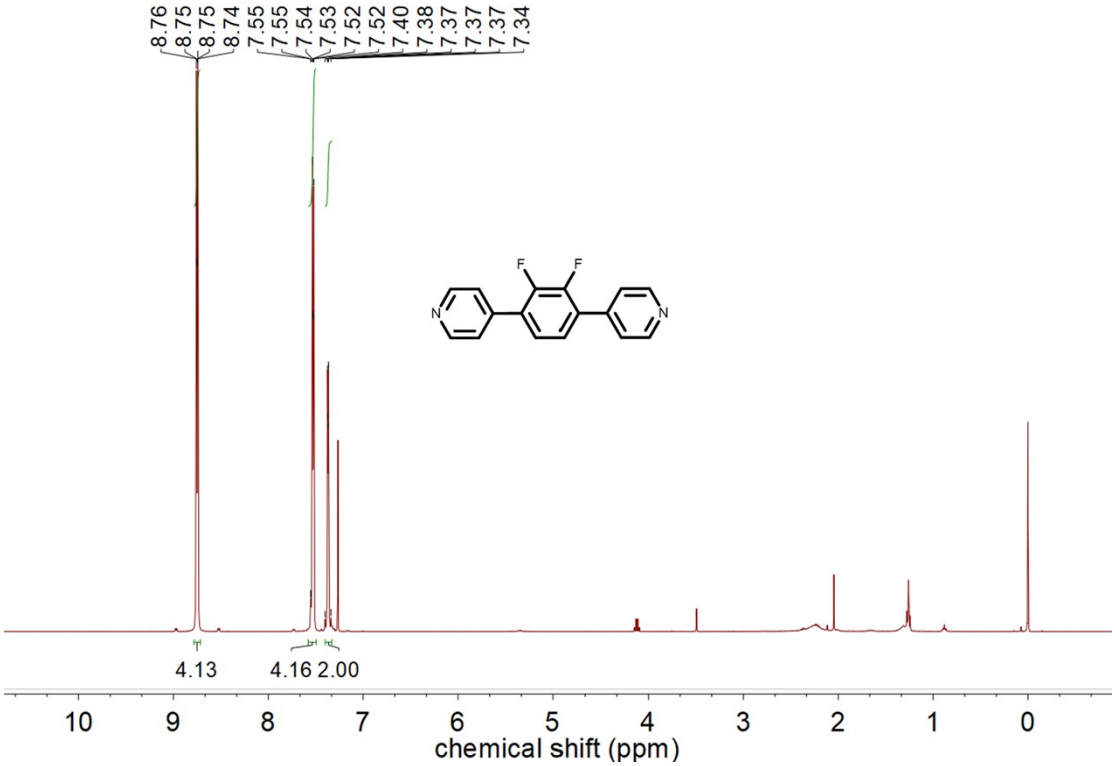

Fig. S8 ^{1}H NMR spectrum of ligand $\mathbf{L_1}$ (500 MHz) in $CDCl_3$.

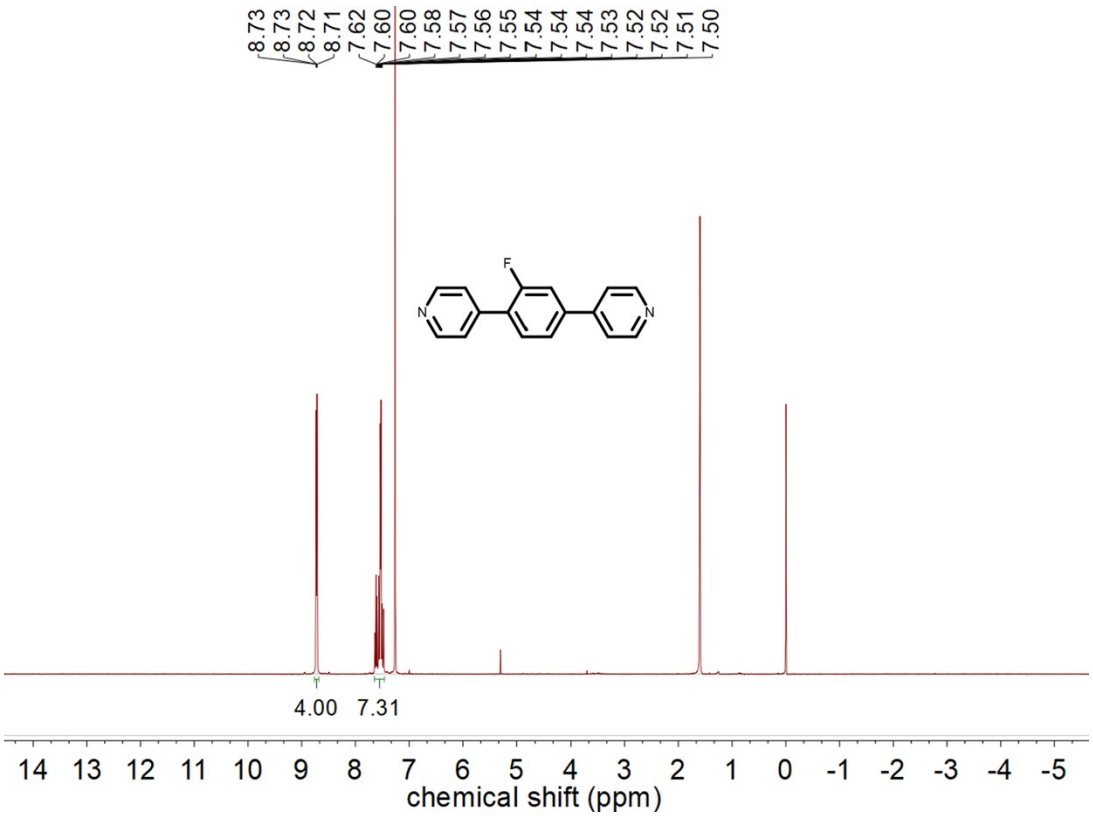

Fig. S9 ^{1}H NMR spectrum of ligand $\mathbf{L_2}$ (500 MHz) in $CDCl_3$.

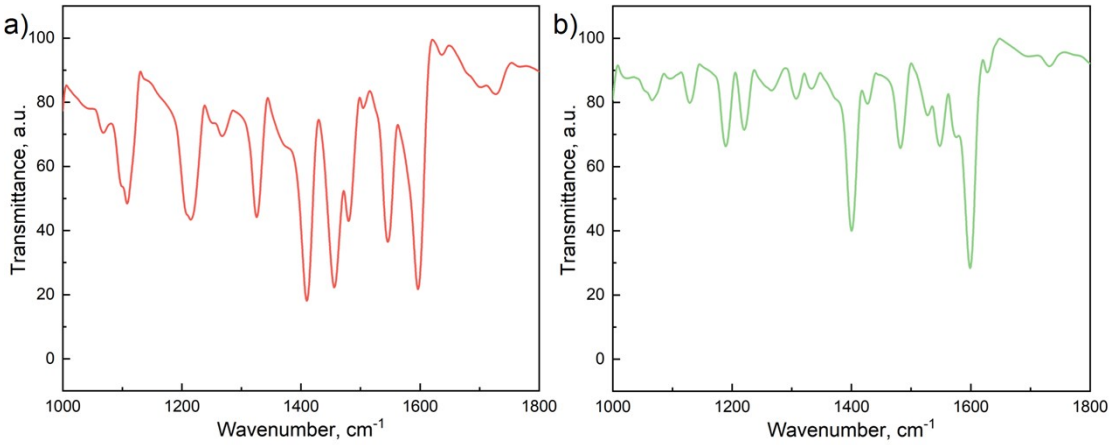

Fig. S10 IR spectra of ligand (a) $\mathbf{L_1}$; (b) $\mathbf{L_2}$.

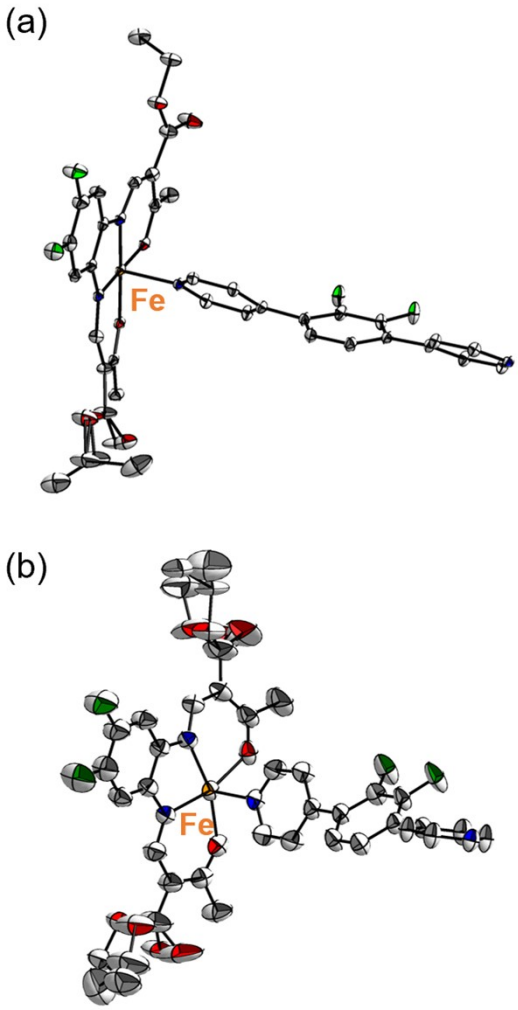

Fig. S11 The asymmetric unit of complex **1** (a) at 120 K; (b) at 300 K. (ORTEP drawing, thermal ellipsoids at a 50% probability level. All the hydrogen atoms and solvents are omitted for clarity).

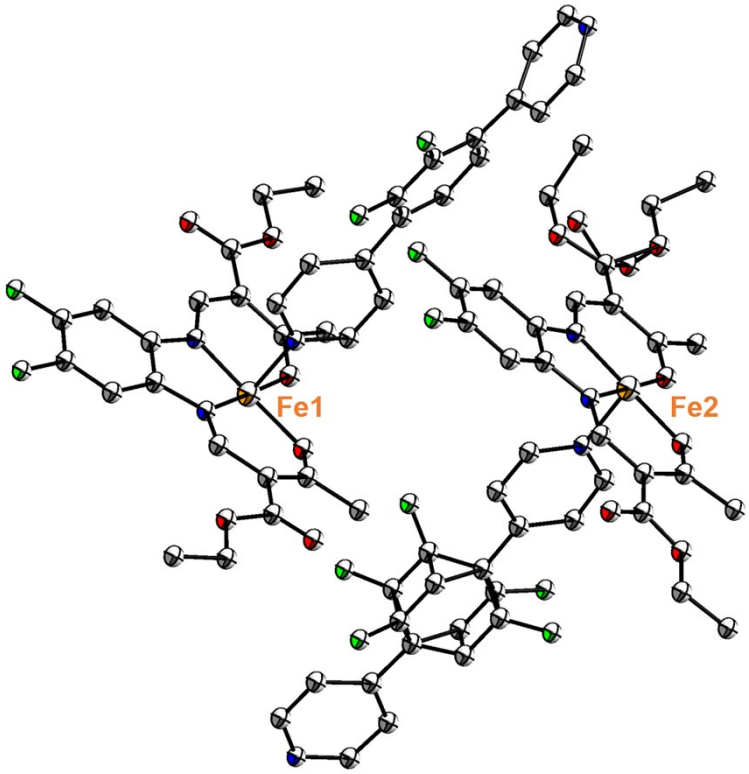

Fig. S12 The asymmetric unit of complex **2** at 120 K. (ORTEP drawing, thermal ellipsoids at a 50% probability level. All the hydrogen atoms and solvents are omitted for clarity).